doi:10.1006/jmbi.2000.3826 available online at http://www.idealibrary.com on IDEAL® J. Mol. Biol. (2000) 300, 93–102

JMB

Alternative Conformations of a Nucleic Acid Four-way Junction

Jacek Nowakowski[1,2], Peter J. Shim[2], C. David Stout[2]* and Gerald F. Joyce[1,2]*

[1]*Department of Chemistry and The Skaggs Institute for Chemical Biology, The Scripps Research Institute, 10550 N. Torrey Pines Road, La Jolla CA 92037, USA*

[2]*Department of Molecular Biology, The Scripps Research Institute, 10550 N. Torrey Pines Road, La Jolla CA 92037, USA*

**Corresponding authors*

A crystal structure of a 108 nucleotide RNA-DNA complex containing a four-way junction was solved at 3.1 Å resolution. The structure of the junction differs substantially from the ''stacked-X'' conformation observed previously, due to a 135° rotation of the branches. Comparison of the two conformers provides insight into the factors contributing to the flexibility of four-way junctions. The stacked-X conformation maximizes base-stacking but causes unfavorable repulsion between phosphate groups, whereas the 135°-rotated ''crossed'' conformation minimizes electrostatic clashes at the expense of reduced base-stacking. Despite the large rotation of the branches, both junction structures exhibit an antiparallel arrangement of the continuous strands and opposite polarity of the crossover strands.

Keywords: crossover isomerization; four-way junction; Holliday junction; nucleic acid structure; recombination

Introduction

Four-way junctions are a common feature of nucleic acid structure and have important biological consequences. A DNA four-way junction, the Holliday junction, is formed during DNA recombination and serves as the primary substrate for various recombination proteins (Holliday, 1964; Voziyanov *et al*., 1999). Four-way junctions also occur in a variety of structured RNAs, including 23 S rRNA (Wimberly *et al*., 1999; Conn *et al*., 1999), U1 snRNA (Branlant *et al*., 1981), genomic RNA of Qβ and MS2 bacteriophage (Beekwilder *et al*., 1995; Poot *et al*., 1997), and the hairpin ribozyme (Hampel & Tritz, 1989).

Experimental evidence suggests that four-way junctions are dynamic structures capable of undergoing large conformational changes. Reported crystal structures of an all-DNA four-way junction complexed with either Cre or RuvA recombinase reveal a substantial change in the angle between the branches at the junction compared to the structure of the unbound junction in solution (Guo *et al*., 1997; Hargreaves *et al*., 1998). Even in the absence of proteins, the Holliday junction can undergo a conformational rearrangement, known as crossover isomerization, in which the two continuous and two crossover strands are exchanged. This rearrangement results in the partial exchange of sister chromatids during DNA recombination and can lead to gene conversion (Kowalczykowski *et al*., 1994). Another aspect of the structural flexibility of the Holliday junction is manifested during branch migration, when the junction propagates along homologous stretches of DNA through dissociation and reassociation of base-pairs (Panyutin *et al*., 1995). The dynamic properties of four-way junctions often have functional significance, for example, in the regulation of translation of viral mRNAs (Poot *et al*., 1997) and in ribozyme catalysis (Walter *et al*., 1998a, 1999).

Despite a growing amount of structural information regarding four-way junctions, their dynamic properties remain poorly understood. The mechanism of crossover isomerization of Holliday junctions had been studied in solution using NMR spectroscopy and fluorescence resonance energy transfer techniques (Miick *et al*., 1997; Overmars & Altona, 1997; Grainger *et al*., 1998; Walter *et al*., 1998b). These studies revealed that the rate of interconversion and the relative abundance of the two junction conformers depend on the nucleotide sequence at the junction and the presence of divalent metal ions in solution. A more detailed struc-

Present address: J. Nowakowski, Department of Chemistry and Biochemistry, University of Texas, Austin, TX 78712, USA.

E-mail addresses of the corresponding authors: dave@scripps.edu; gjoyce@scripps.edu

0022-2836/00/010093–10 $35.00/0

tural view of different conformers of a four-way junction is needed in order to understand the dynamic properties of the junction and the mechanism of crossover isomerization.

During the past year, two crystal structures of all-nucleic-acid four-way junctions were reported. One involved a junction containing two strands of RNA and two strands of DNA that adopted an antiparallel orientation and crossed at a relative angle of 55° (Nowakowski *et al*., 1999a). This structure corresponds to the ''stacked-X'' conformation, which is postulated to exist for DNA junctions in solution in the presence of divalent metal cations (Lilley & Clegg, 1993; Seeman & Kallenbach, 1994). The second crystal structure involved an all-DNA junction, also in an antiparallel orientation and with the strands crossing at a 40° angle (Ortiz-Lombardia *et al*., 1999). The two structures are very similar, enabling one to draw general conclusions about four-way junctions composed of either DNA or RNA (Lilley & Clegg, 1993). Here, a new crystal structure of the RNA-DNA complex is presented, containing the same junction sequence as before, but adopting a conformation in which the branches are rotated by 135° relative to the stacked-X conformation (Figure 1). The new structure reveals a different metal ion binding site formed by nucleotides at the junction, and exhibits a different arrangement of electrostatic and base-stacking interactions. Taken together, the two structures provide insight into the ability of four-way junctions to adopt alternative conformations, as required for DNA recombination.

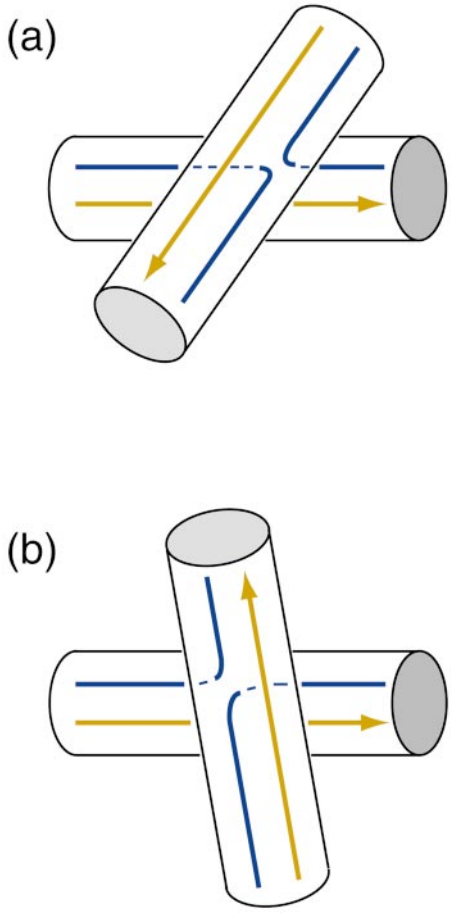

Figure 1. A diagram showing the overall structural features of the two junction conformations. (a) The stacked-X conformation; (b), the crossed conformation. The continuous strands are indicated by gold lines and the crossover strands by blue lines.

Results

Structure of the complex

The RNA-DNA complex described here contains 108 nucleotides (34,000 Da), located within two strands of DNA and two strands of RNA (Figure 2(a)). The four strands form three double-helical domains: two RNA-DNA domains and one DNA-DNA domain. Each RNA-DNA domain contains 20 base-pairs, divided into helices of 9 and 11 bp that are coaxially stacked. Residues A10 and G31, at the end of the 11 bp helix, form a non-standard pair. The RNA-DNA domains adopt an *A*-form helical conformation. The DNA-DNA domain contains eight continuous base-pairs that connect the two RNA-DNA domains and adopt a *B*-form conformation. The overall secondary structure of the complex is the same as that of the stacked-X complex described previously (Nowakowski *et al*., 1999a), differing only by the length of the RNA-DNA domains. Both structures exhibit 2-fold symmetry, although this symmetry is non-crystallographic in the new structure.

The new structure exhibits two four-way junctions, formed between the RNA-DNA and DNA-DNA portions of the complex that are positioned at a relative angle of 80°. The complex has an overall triangular shape, with the three double-helical domains lying nearly orthogonal to one another (Figure 2(b) and (c)). The non-crystallographic 2-fold symmetry axis passes through the center of the DNA-DNA duplex, perpendicular to its long axis. The symmetry of the two halves of the molecule is broken within the hairpin loops that close the ends of the DNA-DNA duplex and by the differential positioning of bound metal ions. The overall dimensions of the complex are 50 Å × 60 Å × 45 Å.

The four-way junction

The four-way junction is formed by residues G9, A10, G31, G32, C137, T138, A145, and C146, and by their 2-fold symmetry mates (Figure 3(c) and (d)). All nucleotides at the junction are base-paired in a standard Watson-Crick manner, except the non-canonical pair formed between nucleotides A10 and G31. A similar A-G pair was observed in the crystal structure of an all-DNA four-way junction (Ortiz-Lombardia *et al*., 1999). The crossover

strands (nucleotides A30-C33 and A145-T147) are of opposite polarity and form sharp turns of the phosphodiester backbone between nucleotides G31 and G32, and between nucleotides A145 and C146. The continuous strands are antiparallel as well and run almost orthogonally. The four-way junction positions the stacked helical branches at a relative angle of 80° (Figure 3(c)). This orientation is rotated by 135° relative to the stacked-X conformation (Figure 3(a)).

The crystal structure of the 135°-rotated junction contains 14 peaks in the $|F_{obs}| - |F_{calc}|$ difference Fourier map, ranging in intensity from 3σ to 8σ, that do not correspond to nucleic acid. This extra density can be assigned to bound magnesium hexahydrate ions, based on the geometry of coordination to nearby ligands and the composition of the crystallization mixture. One of the hydrated metal ions coordinates to nucleotides that form the junction (Figure 3(d)). This metal ion is located in the major groove of the RNA-DNA domain at the interface between helices 3 and 4. It exhibits three outer-sphere contacts (3.5-4.5 Å) to the keto oxygen atoms of G9 and G31, and the amino group of A10.

Comparison of the stacked-X and 135°-rotated structures

The previously reported crystal structure of a smaller, 82 nucleotide RNA-DNA complex demonstrated a four-way junction in which the branches were stacked at a relative angle of 55° (Nowakowski *et al*., 1999a). This is referred to as the stacked-X conformation. The primary and secondary structures of the stacked-X and the 135°-rotated junctions are the same. There are large differences, however, in their overall conformation (Figure 1). Figure 3(a) and (c) show the nomenclature for the four helices that form the two junction structures. Helices 1 and 2 form the DNA-DNA domain, and helices 3 and 4 form the two RNA-DNA domains. The angle between the axis of helices 1 and 2 and the axis of helices 3 and 4 is defined as the junction branch angle. From this frame of reference, the inter-branch angle of the previously reported structure is +55° and that of the current structure is −80°. Therefore, the two structures represent distinct conformations of the same four-way junction, related to each other by a 135° rotation of the stacked branches. For simplicity, the 135°-rotated structure is referred to as the crossed conformation, based on the near-perpendicular arrangement of the two helical axes.

All base-pairs in the stacked-X junction are involved in base-stacking interactions within a standard double helix (Figures 3(b) and 4(a)). This base-stacking is continuous across the sites of coaxial stacking between helices 1 and 2, and between helices 3 and 4. In the crossed junction, the 135° rotation results in disruption of base-stacking between helices 3 and 4. The bases of nucleotides G31 and C146 are rotated away from each other by 30° and are no longer fully stacked (Figure 4(c)). The geometry of the A10-G31 pair also is different in the two conformers, buckling from planarity by about 15° in the crossed conformation. This disruption of base-stacking, however, is limited to base-pairs G9-C146 and A10-G31 at the interface between helices 3 and 4. The stacking arrangement of base-pairs in helices 1 and 2 is unperturbed.

The two junction conformations differ significantly in the phosphate-phosphate distances between residues that form the crossover strands. In the +55° stacked-X junction, the sharp angle between the branches creates two close contacts between phosphate groups of residues G32 and G33, and residues C146 and T147 (Table 1). The phosphate-phosphate distances for these two nucleotide pairs are 5.0 and 5.1 Å, respectively, corresponding to a direct van der Waals contact (Figure 4(b)). Such close proximity between negatively charged groups creates unfavorable electrostatic repulsion, which is expected to destabilize the stacked-X conformation. In the −80° crossed junction, the distances between the G32-C33 and C146-T147 phosphate groups are increased to 6.5 and 5.8 Å, respectively, placing them at distances that are more typical for phosphate groups in nucleic acid double-helices (Figure 4(d)).

In the stacked-X junction, a cobalt hexamine complex binds in the minor groove of helix 1, coordinating to nucleotides that form the sharp angle between the branches (Nowakowski *et al*., 1999a). This coordination involves outer-sphere interactions within the major groove of helix 1 and with phosphate groups of helix 4 (Figures 3(a) and (b), and 4(b)). The location of the cobalt ion implies a corresponding role for $[Mg(H_2O)_6]^{2+}$ in reducing electrostatic repulsion between the phosphate groups of G32 and C33. In contrast, no metal ions were observed in the crossed junction between the crossed branches of helices 1 and 4. Instead, a hydrated magnesium ion was seen in the major groove of the RNA-DNA domain at the interface between helices 3 and 4 (Figures 3(c) and (d), and 4(d)). This magnesium ion engages in outer sphere coordination with base-paired nucleotides at the site of disrupted stacking caused by the rotation of helices 3 and 4 (Figure 4(c)). Distortion of the regu-

Table 1. Phosphate-phosphate distances between nucleotides at the junction

Nucleotide pairs	+55° junction	−80° junction
A30-G31	6.31	5.69
G31-G32	6.60	6.75
G32-C33	**4.96**	6.45
G31-A145	6.83	15.11
G32-C146	6.24	6.18
G144-A145	6.92	6.65
A145-C146	6.65	6.92
C146-T147	**5.09**	5.81

Distances are in Å; those shorter than 5.5 Å are shown in bold.

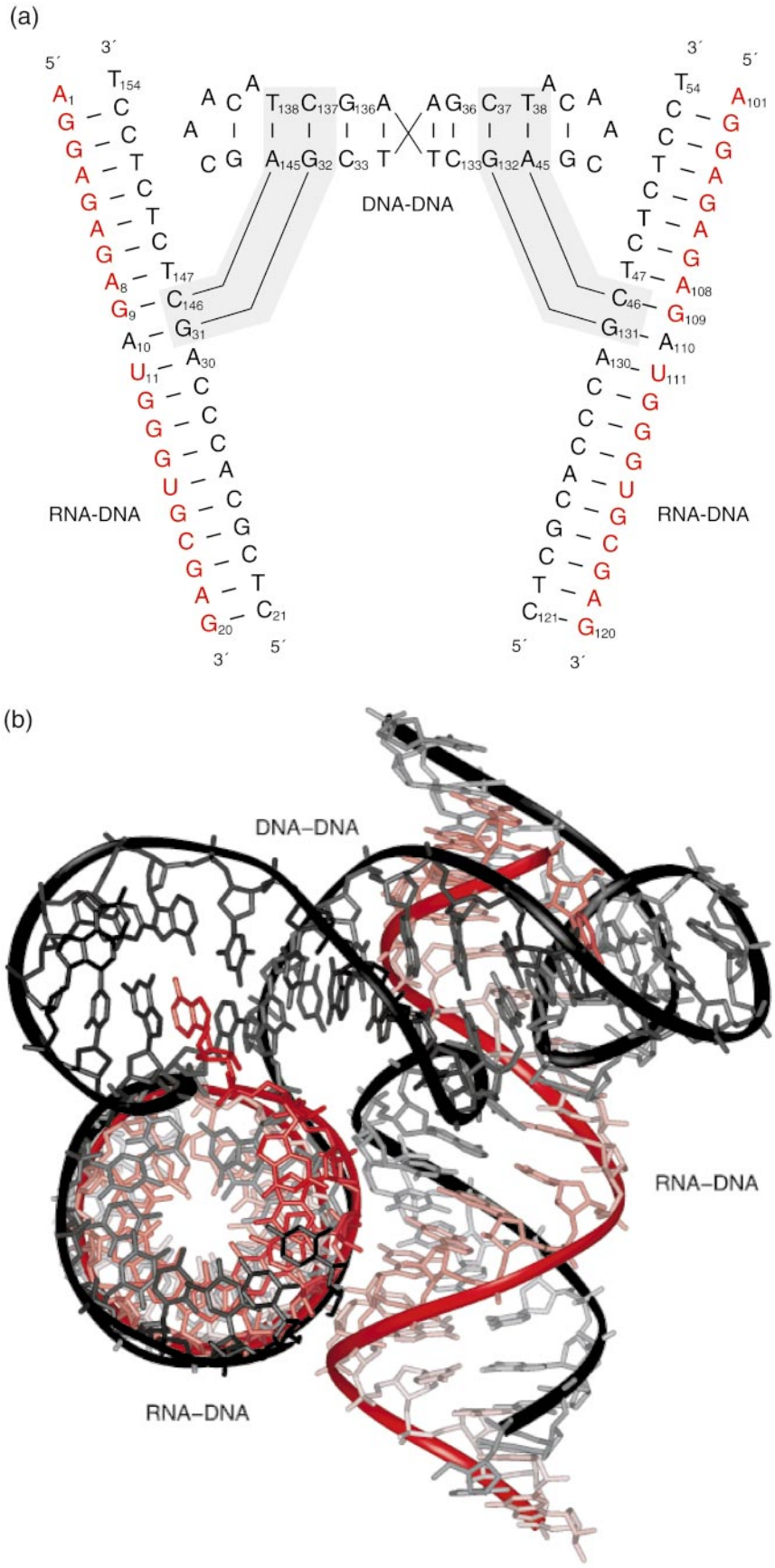

Figure 2 (*legend opposite*)

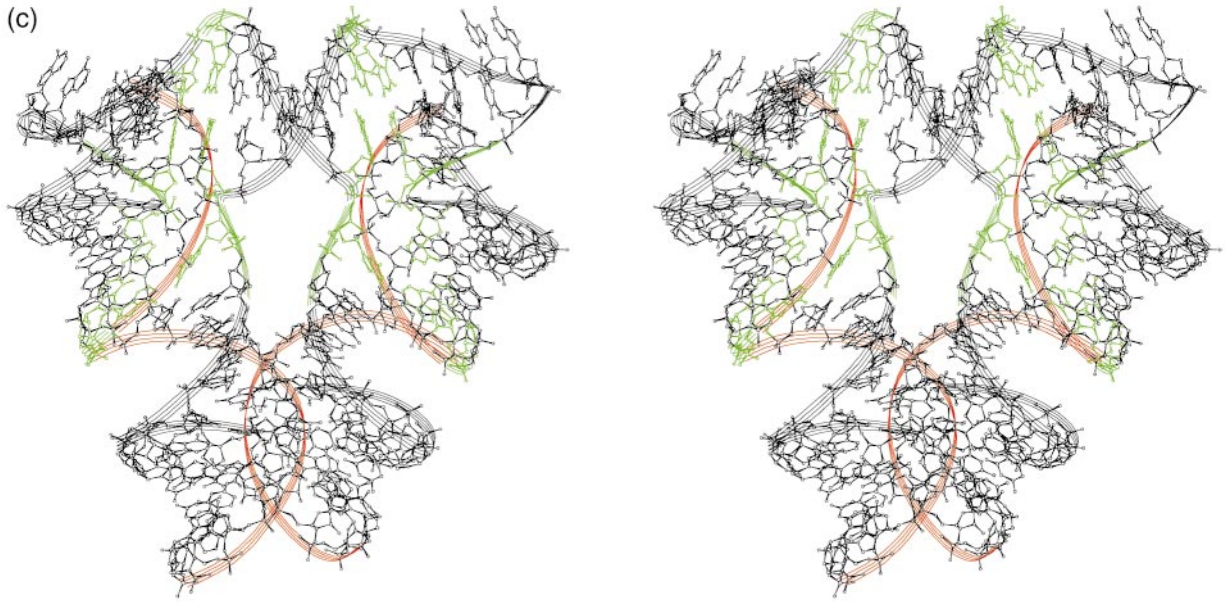

Figure 2. Structure of the 108 nucleotide RNA-DNA complex. (a) Secondary structure and numbering scheme of the RNA-DNA complex. RNA residues are in red and DNA residues are in black. The two non-crystallographic, symmetry-related four-way junctions are highlighted by the shaded areas. (b) Three-dimensional structure of the RNA-DNA complex as viewed down the long axis of one of the RNA-DNA helices. This arrangement shows the orthogonal positioning of the three double-helical domains. (c) Stereo view of the RNA-DNA complex. Nucleotides forming the four-way junctions are in green and the RNA backbone is in red.

lar *A*-form helical geometry between the G9-C146 and A10-G31 pairs brings the keto oxygen atoms of G9 and G31 close together, thereby creating a binding site for the metal ion. It appears that the bound magnesium ion stabilizes the distorted geometry of the poorly stacked interface between helices 3 and 4.

Discussion

Conformational variability is an important feature of four-way junctions. The inter-branch angles of the Holliday junction change during the course of recombination, facilitating branch migration, formation of crossover isomers, and resolution of the junction. The two crystal structures discussed in this study provide a detailed structural view of two distinct conformers of the same four-way junction (Figure 1). These structures illustrate the extent to which the branches of the junction can be rotated without disrupting the overall secondary structure, and reveal energetic factors that are involved in the transition between the two junction conformers. Both structures are compatible with coaxial extension of the four component helices, based on modeling studies.

The 135° rotation of the junction branches is achieved by reversing the trade-off between base-stacking interactions and electrostatic contacts that involve phosphate groups and bound metal ions. In the +55° stacked-X conformation, base-stacking is maximized and resembles the stacking interaction of a standard double helix (Figure 4(a)). The stabilizing effect of base-stacking is offset by electrostatic repulsion between closely spaced phosphate groups, compensated in part by a metal cation bound near the sharp turn of the phosphodiester backbone (Figures 3(b) and 4(b)). In the −80° crossed conformation, electrostatic repulsion is significantly reduced because the phosphate-phosphate distances are increased (Figure 4(d)), but there is much weaker base-stacking among the nucleotides at the junction (Figure 4(c)). The weaker stacking interactions are compensated by metal ion interactions, occurring at a different site than in the stacked-X conformation (Figure 3(d)).

Solution studies of the crossover isomerization process have indicated that the relative amounts of the two crossover conformers is highly dependent on the nucleotide sequence surrounding the branch site and on the presence of divalent metal cations (Miick *et al.*, 1997; Grainger *et al.*, 1998). The two structures of a four-way junction presented here demonstrate that even those nucleotides that do not participate directly in forming the junction may be involved in forming metal-binding sites that help to stabilize the junction structure. In the stacked-X conformation, the metal binds to the first and second base-pairs of helix 1 (Figure 3(a) and (b)), while in the crossed conformation the metal binds in the major groove at the interface between helices 3 and 4 (Figure 3(c) and (d)). Therefore, the movement of the branches during crossover isomerization is likely to be accompanied by the binding and release of metal ions as electrostatic forces change during branch rotation. Because most of

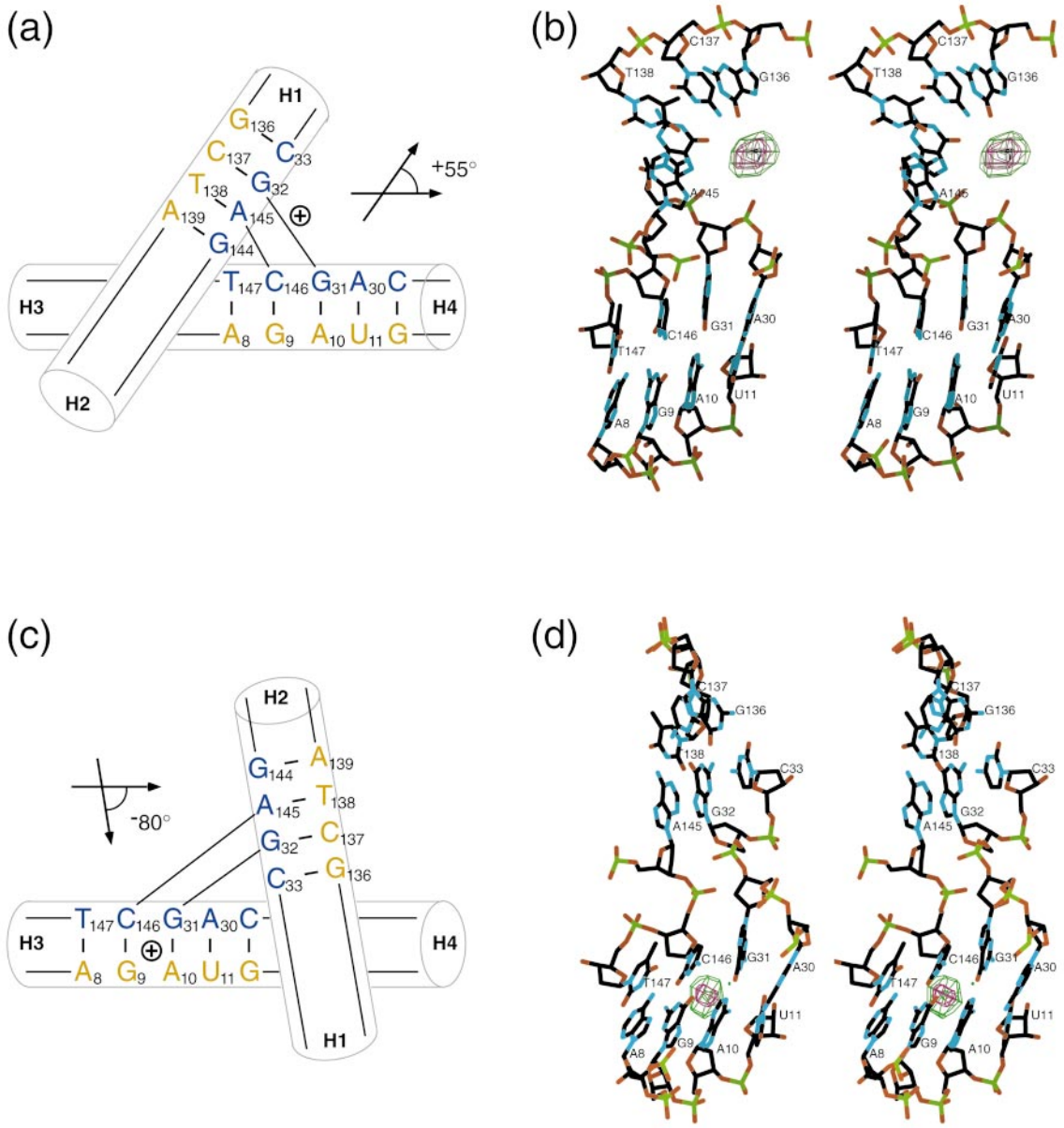

Figure 3. Structures of the two different conformations of the four-way junction. (a) and (b) The +55° stacked-X conformation as seen in the previously solved crystal structure of an 82 nucleotide RNA-DNA complex (Nowakowski *et al.*, 1999a). (c) and (d) The −80° crossed conformation as seen in the present structure. (a) and (c) Diagram of the secondary structure of the junction showing the connectivity of the branches. The location of a bound metal ion is indicated by a circled plus sign. Helices 1-4 are labeled H1-H4, respectively. (b) and (d) Stereo views of the two conformations. The locations of bound metals are shown as $|F_{obs}| - |F_{calc}|$ difference electron density, contoured at 6σ (black), 5σ (magenta), and 4σ (green).

the metal ion contacts seen in the crystal structures involve coordination to nucleotide bases, different sequences at the junction will have a different propensity to bind the metal and therefore a sequence-specific effect on the relative abundance of the two crossover conformers.

Previous studies of RNA four-way junctions, involving comparative gel electrophoresis and fluorescence resonance energy transfer analysis, demonstrated that the same junction could adopt two different conformations, depending on the concentration of divalent metal cations (Walter *et al.*, 1998b). At high Mg^{2+} concentrations (>1 mM) the junction adopted a structure corresponding to the stacked-X conformation, while at low Mg^{2+} concentrations (<0.1 mM) it more closely resembled the crossed conformation. These alternative conformers were not observed for an all-DNA junction, which became unstacked at low Mg^{2+} concentrations (Duckett *et al.*, 1988). Conversely, a different RNA four-way junction, derived from U1 snRNA, remained in the crossed conformation even at high Mg^{2+} concentrations (Walter *et al.*, 1998b). The nucleic acid four-way junction

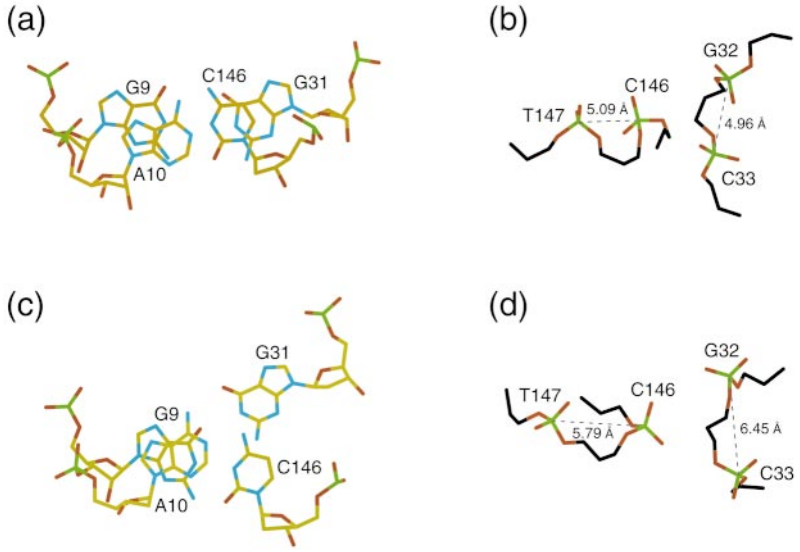

Figure 4. Detailed structural differences between (a) and (b) the stacked-X conformation, and (c) and (d) the crossed conformations of the four-way junction. (a) and (c) Stacking arrangement between the G9-C146 and A10-G31 base-pairs, which lie at the interface of helices 3 and 4. (b) and (d) Inter-phosphate distances between residues G32 and C33, and between residues C146 and T147.

described here can adopt either conformation at high Mg^{2+} concentrations within the context of the crystal lattice.

Despite the large difference in the inter-branch angle, both junction conformers exhibit an antiparallel arrangement of the continuous strands. In the presumed transition between conformers, nearly all of the change in the inter-branch angle would be accommodated by changes in the torsion angles at the pivotal phosphodiester linkages (Table 2). The additional branch rotation necessary to switch the junction polarity and accomplish crossover isomerization would further disrupt base-stacking at the interface between helices 3 and 4, and likely compromise the integrity of the coaxial stack. Nonetheless, this structural change appears to be allowed because of the ability of the sugar-phosphate backbone to adopt multiple, stable conformations. The crystal structures of the four-way junction in the stacked-X and crossed conformations suggest that electrostatic repulsion sets the lower limit of the inter-branch angle in the stacked-X conformation, while the loss of base-stacking defines this angle in the crossed conformation. These counterbalancing influences, in concert with the stabilizing effect of metal ions that are bound at specific sites that are unique to each conformer, are expected to control the processes of branch migration and crossover.

Materials and Methods

Sample preparation, crystallization, and data collection

The sequences of the DNA and RNA strands used in crystallization of the four-way junction correspond to the sequences of the 10-23 DNA enzyme and its RNA substrate (Santoro & Joyce, 1997). RNA residues A10 and A110 were substituted with deoxyadenylate to prevent DNA-catalyzed cleavage of the RNA strand. DNA oligonucleotides were obtained from Operon Technologies (Alameda, CA) and RNA oligonucleotides were synthesized on a Pharmacia LKB Gene Assembler Special from commercially available phosphoramidites (Pharmacia). All oligonucleotides were purified as described (Nowakowski *et al.*, 1999a). The particular sequence of the RNA-DNA complex used for crystal structure determination was identified through a combinatorial sequence screen (Nowakowski *et al.*, 1999b). Crystals were grown at 24.5 °C from 50 mM sodium cacodylate (pH 6.0), 20 mM $MgCl_2$, 1 mM spermine, and 25 % (v/v) methyl-2,4-pentanediol (MPD) using the vapor diffusion method. The complex crystallized in space group *I*222; $a = 62.81$ Å, $b = 114.26$ Å, and $c = 171.45$ Å. All data sets were collected at the Stanford Synchrotron Radiation

Table 2. Dihedral angles for phosphodiester linkages at the junction

	G31-G32		A145-C146	
Torsion angle	+55 ° junction	−80 ° junction	+55 ° junction	−80 ° junction
ε	−118	−142	**−91**	**−152**
ζ	**−59**	**+167**	**−92**	**+84**
α	**−94**	**+31**	+87	+55
β	**−138**	**+125**	+137	+174
γ	+51	+92	**−59**	**+55**

Angles that differ by more than 2σ between the two structures are shown in bold.

Table 3. Data collection and phase determination

Data set	Native	E288	E289	E291
Heavy atom	-	I-T22	I-T38	I-T51
X-ray source	SSRL 7-1	SSRL 7-1	SSRL 7-1	SSRL 7-1
Wavelength (Å)	1.08	1.08	1.08	1.08
Max. res. (Å)	3.1	3.1	3.1	3.1
Completeness (%)				
Overall	99.2	99.7	98.3	99.3
High res. bin	99.2	99.7	98.2	99.2
I/σ (I)				
Overall	7.1	6.4	7.0	7.2
High res. bin	2.0	1.9	1.9	2.0
Multiplicity	4.2	3.9	4.0	4.0
Reflections	13,935	13,467	13,845	13,424
$R_{sym}(I)$[a] (%)	5.1	5.8	5.5	5.3
Phasing power[b]	-	0.91	0.81	1.37
Combined figure of merit	0.419			
Refinement				
Resolution (Å)	20.0-3.1			
Reflections[c]	10,948			
Atoms				
Nucleic acid	2240			
Hydrated metals	14			
Water	0			
$R^{c,d}_{cryst}$	22.6			
R^{e}_{free} (10 % data)	25.8			
Geometry				
r.m.s. deviation bonds (Å)	0.011			
r.m.s. deviation angles (deg.)	1.272			
r.m.s. deviation dihedrals (deg.)	28.9			

[a] $R_{sym}(I) = \Sigma_{hkl}\ \Sigma_i\ |I_{hkl,i} - \langle I_{hkl}\rangle| / \Sigma_{hkl}\ \Sigma_i\ |I_{hkl,i}|$, where $\langle I_{hkl}\rangle$ is the mean intensity of the multiple $I_{hkl,i}$ observations for symmetry-related reflections.

[b] Phasing power $= \langle f_H\rangle / \langle E\rangle$, where f_H is calculated heavy-atom structure amplitude, E is the lack of closure error.

[c] $|F| > 2\sigma(F)$.

[d] $R_{cryst} = \Sigma_{hkl}\ ||F_{obs}| - |F_{calc}|| / \Sigma_{hkl}\ |F_{obs}|$.

[e] $R_{free} = \Sigma_{hkl\varepsilon T}\ ||F_{obs}| - |F_{calc}|| / \Sigma_{hkl\varepsilon T}\ |F_{obs}|$, where the test set T includes 10 % of the data.

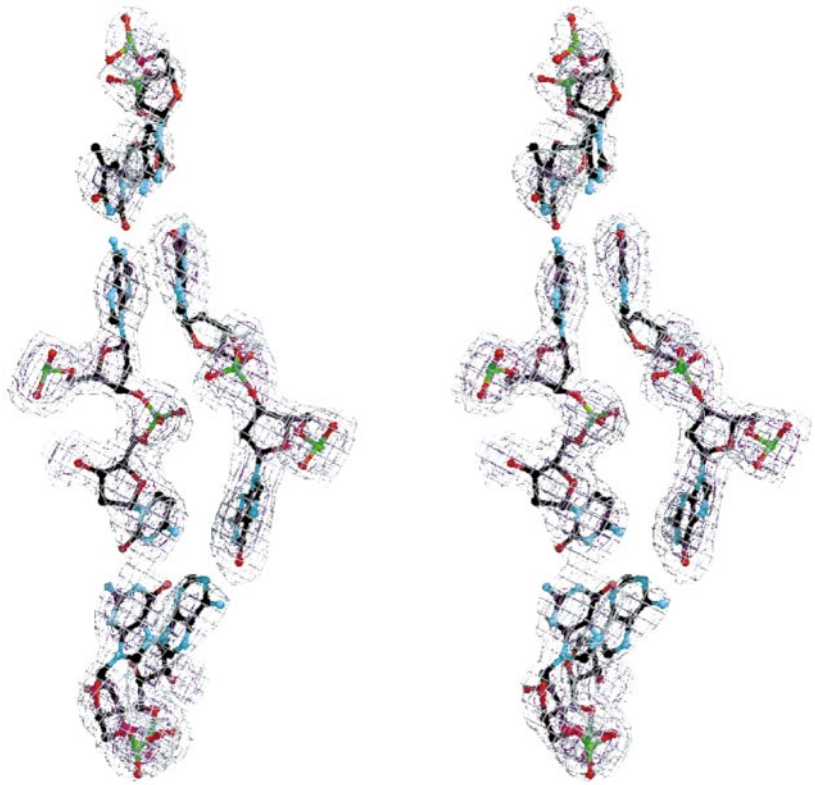

Figure 5. Stereo view of electron density for the eight nucleotides that form the four-way junction in the -80° crossed conformation. The map was calculated using all data in the resolution range 27.0-3.1 Å with σ_A-weighted coefficients $2m|F_{obs}| - D|F_{calc}|$, contoured at 1σ (gray) and 3σ (purple). The view of the junction is similar to that shown in Figure 3(d), with residue C137 at the top and residues G9 and A10 at the bottom.

Laboratory beamline 7-1 (Table 3). Prior to data collection, crystals were flash frozen at 100 K directly from the mother liquor. Data sets were integrated with MOSFLM and scaled with SCALA (CCP4, 1994).

Structure determination and refinement

The structure of the complex was determined by multiple isomorphous replacement using three heavy-atom derivatives (Table 3). All derivatives were prepared by incorporating 5-iodo-substituted thymidine residues within the DNA strand. The positions of heavy-atom sites were determined with SOLVE (Terwilliger & Berendzen, 1999). The refinement of heavy atom positions and calculation of multiple isomorphous replacement (MIR) phases were carried out with MLPHARE (CCP4, 1994). The experimental density was solvent-flattened with DM (CCP4, 1994). The initial electron density maps were generated with and without NCS averaging (X-PLOR 3.8). The two maps used in combination enabled unambiguous tracing of the entire phosphodiester backbone. The model was built from individual nucleoside monophosphates and fitted to the electron density using Xtalview (McRee, 1999). Refinement of the structure was carried out with XPLOR 3.8 (Brünger, 1993) and consisted of cycles of positional refinement, bulk solvent correction, overall anisotropic scaling, and manual refitting of the model (Figure 5). NCS averaging constraints were not used during the refinement. When the *R*-factor dropped to 27.5 % ($R_{free} = 31.0$ %), grouped *B* refinement was performed assuming three groups per nucleotide; phosphate, ribose, and base. This procedure lowered the *R*-factor to 22.7 % ($R_{free} = 25.1$ %). The final model contained 108 nucleotides and 14 magnesium hexahydrate ions. Figures were prepared with InsightII (Biosym) and Xfit (McRee, 1999).

Accession number

The coordinates of the 108-nucleotide RNA-DNA complex have been deposited in the RCSB Protein Data Bank with accession code 1EGK.

Note added in proof

Another crystal structure of an all-DNA four-way function was reported (Eichman, B. F., Vargason, J. M., Mooers, B. H. M. & Ho, P. S. (2000). *Proc. Natl Acad. Sci. USA*, **97**, 3971-3976). This function contains all Watson-Crick base-pairs and adopts a function angle of 41.4°. It is substantiall similar to the stacked-X conformation described previously.

Acknowledgments

The authors thank the staff at the Stanford Synchrotron Radiation Laboratory for their generous assistance. This work was funded by The Skaggs Institute for Chemical Biology of The Scripps Research Institute.

References

Beekwilder, M. J., Nieuwenhuizen, R. & van Duin, J. (1995). Secondary structure model for the last two domains of single-stranded RNA phage Qβ. *J. Mol. Biol.* **247**, 903-917.

Branlant, C., Krol, A. & Ebel, J. P. (1981). The conformation of chicken, rat and human U1A RNAs in solution. *Nucl. Acids Res.* **9**, 841-858.

Brünger, A. T. (1993). *X-PLOR 3.1: A System for Crystallography and NMR*, Yale University Press, New Haven.

CCP4 (1994). The CCP4 suite: programs for protein crystallography. *Acta Crystallog. sect. D*, **50**, 760-763.

Conn, G. L., Draper, D. E., Lattman, E. E. & Gittis, A. G. (1999). Crystal structure of a conserved ribosomal protein-RNA complex. *Science*, **284**, 1171-1174.

Duckett, D. R., Murchie, A. I. H., Diekmann, S., von Kitzing, E., Kemper, B. & Lilley, D. M. J. (1988). The structure of the Holliday junction and its resolution. *Cell*, **55**, 79-89.

Grainger, R. J., Murchie, A. I. H. & Lilley, D. M. J. (1998). Exchange between stacking conformers in a four-way DNA junction. *Biochemistry*, **37**, 23-32.

Guo, F., Gopaul, D. N. & van Duyne, G. D. (1997). Structure of Cre recombinase complexed with DNA in a site-specific recombination synapse. *Nature*, **389**, 40-46.

Hampel, A. & Tritz, R. (1989). RNA catalytic properties of the minimum (−)sTRSV sequence. *Biochemistry*, **28**, 4929-4933.

Hargreaves, D., Rice, D. W., Sedelnikova, S. E., Artymiuk, P. J., Lloyd, R. G. & Rafferty, J. B. (1998). Crystal structure of *E. coli* RuvA with bound DNA Holliday junction at 6 Å resolution. *Nature Struct. Biol.* **5**, 441-446.

Holliday, R. (1964). A mechanism for gene conversion in fungi. *Genet. Res.* **5**, 282-304.

Kowalczykowski, S. C., Dixon, D. A., Eggleston, A. K., Lauder, S. D. & Rehrauer, W. M. (1994). Biochemistry of homologous recombination in *Escherichia coli*. *Microbiol. Rev.* **58**, 401-465.

Lilley, D. M. J. & Clegg, R. M. (1993). The structure of the four-way junction in DNA. *Annu. Rev. Biophys. Biomol. Struct.* **22**, 299-328.

McRee, D. E. (1999). XtalView/Xfit - a versatile program for manipulating atomic coordinates and electron density. *J. Struct. Biol.* **125**, 156-165.

Miick, S. M., Fee, R. S., Millar, D. P. & Chazin, W. J. (1997). Crossover isomer bias is the primary sequence-dependent property of immobilized Holliday junctions. *Proc. Natl Acad. Sci. USA*, **94**, 9080-9084.

Nowakowski, J., Shim, P. J., Prasad, G. S., Stout, C. D. & Joyce, G. F. (1999a). Crystal structure of an 82-nucleotide RNA-DNA complex formed by the 10-23 DNA enzyme. *Nature Struct. Biol.* **6**, 151-156.

Nowakowski, J., Shim, P. J., Joyce, G. F. & Stout, C. D. (1999b). Crystallization of the 10-23 DNA enzyme using a combinatorial screen of paired oligonucleotides. *Acta Crystallog. sect. D*, **55**, 1885-1892.

Ortiz-Lombardía, M., González, A., Eritja, R., Aymamí, J., Azorín, F. & Coll, M. (1999). Crystal structure of a DNA Holliday junction. *Nature Struct. Biol.* **6**, 913-917.

Overmars, F. J. J. & Altona, C. (1997). NMR study of the exchange rate between two stacked conformers of a model Holliday junction. *J. Mol. Biol.* **273**, 519-524.

Panyutin, I. G., Biswas, I. & Hsieh, P. (1995). A pivotal role for the structure of the Holliday junction in DNA branch migration. *EMBO J.* **14**, 1819-1826.

Poot, R. A., Tsareva, N. V., Boni, I. V. & van Duin, J. (1997). RNA folding kinetics regulates translation of

phage MS2 maturation gene. *Proc. Natl Acad. Sci. USA,* **94**, 10110-10115.
Santoro, S. W. & Joyce, G. F. (1997). A general purpose RNA-cleaving DNA enzyme. *Proc. Natl Acad. Sci. USA,* **94**, 4262-4266.
Seeman, N. C. & Kallenbach, N. R. (1994). DNA branched junctions. *Annu. Rev. Biophys. Biomol. Struct.* **23**, 53-86.
Terwilliger, T. C. & Berendzen, J. (1999). Automated MAD and MIR structure solution. *Acta Crystallog. sect. D,* **55**, 849-861.
Voziyanov, Y., Shailja, P. & Jayaram, M. (1999). A general model for site-specific recombination by the integrase family recombinases. *Nucl. Acids Res.* **27**, 930-941.
Walter, F., Murchie, A. I. H. & Lilley, D. M. J. (1998a). The folding of the four-way RNA junction of the hairpin ribozyme. *Biochemistry,* **37**, 17629-17636.
Walter, F., Murchie, A. I. H., Duckett, D. R. & Lilley, D. M. J. (1998b). Global structure of four-way junctions studied using fluorescence resonance energy transfer. *RNA,* **4**, 719-728.
Walter, N. G., Burke, J. M. & Millar, D. P. (1999). Stability of hairpin ribozyme tertiary structure is governed by the interdomain junction. *Nature Struct. Biol.* **6**, 544-549.
Wimberly, B. T., Guymon, R., McCutcheon, J. P., White, S. W. & Ramakrishnan, V. (1999). A detailed view of a ribosomal active site: the structure of the L11-RNA complex. *Cell,* **97**, 491-502.

Edited by J. Doudna

(Received 17 February 2000; received in revised form 24 April 2000; accepted 28 April 2000)